Filtration of oil from oily wastewater via hydrophobic modified quartz sand filter medium

Wei Bigui, Liu Jianlin, Wang Gang and Chang Qing

ABSTRACT

To improve the hydrophobicity and lipophilicity of a quartz sand filter medium, two coupling agents, DN101 and KH570, were employed. The filter medium surface wettability and oil removal efficiency before and after modification were investigated, and the characteristics are summarized. The test results show that, after modification by the grafting of an organic long-chain coupling agent to the filter medium surface, the Lipophilic to Hydrophilic Ratio increased from 1.31 (UQS) to 12.09 (MQD-Ti) and 5.11 (MQD-Si), and the oil removal efficiencies of MQD-Ti and MQD-Si improved by 21.7% and 6.9%, respectively. The stronger hydrophobicity resulted in higher quality factor values of 0.668 m^{-1} and 0.548 m^{-1} for MQD-Ti and MQD-Si, respectively, compared to 0.533 m^{-1} for UQS. This means that improving the filter medium surface hydrophobicity and oil removal efficiency via filter medium surface modification is effective.

Key words | coupling agent, filtration, oily wastewater, quartz sand filter medium, surface modification

Wei Bigui (corresponding author)
Liu Jianlin
Wang Gang
Chang Qing
School of Environmental and Municipal Engineering,
Lanzhou Jiaotong University,
Lanzhou, Gansu 730070,
PR China
E-mail: *weibigui@yahoo.com*

INTRODUCTION

Numerous industries, such as the food, metal, transport, textile and petrochemical industries, produce large amounts of oily wastewater (Jamaly *et al.* 2015), which has a complex composition and a wide range of concentrations and is hazardous to the environment in various ways (Mueller *et al.* 1997). Current common oily wastewater disposal methods include gravity separation, dissolved air flotation, chemical treatment, coalescence, membrane treatment and biological treatment (Kota *et al.* 2012; Li *et al.* 2016; Mazumdar *et al.* 2017; Ngang *et al.* 2017). However, there are numerous issues: the processing efficiencies of these methods are low; the processing facilities require a large area, are expensive, or require complex operations; there are strict requirements on the concentration of the oily wastewater inflow; and the equipment is susceptible to clogging. Filtration is also commonly applied in secondary and tertiary sewage treatment (Hamoda *et al.* 2004; Kratochvil *et al.* 2017). After this treatment, the oily wastewater meets relevant standards and can be discharged or recycled.

A deep bed filter may remove particle sizes smaller than the filter pore size (Takahashi *et al.* 1979; Bai & Tien 2000) due to adsorption to the surface of the filter medium. Therefore, the physical chemical interaction between the pollutant and filter medium is the major factor influencing pollutant removal (Bai & Tien 1997). In general, if the granular filter medium surface has strong hydrophobicity, it also has strong lipophilicity and a superior capability to remove hydrophobic pollutants such as oil. On the other hand, if the filter surface has weak hydrophobicity, it has weak lipophilicity and an inferior oil removal capability (Shin & Chase 2004). Therefore, to improve oil-water separation efficiency from oily wastewater by the filtration process, the filter medium surface can be modified to improve its hydrophobicity.

doi: 10.2166/wrd.2018.052

Zhou *et al.* (2010) employed a quaternary ammonium surfactant to modify a polystyrene resin's surface and improved the oil removal efficiency by 15.5%. Huang & Lim (2006) employed a hydrophobic-oleophilic kapok filter to treat oily wastewater and achieved a removal rate of 99%. Wei *et al.* (2013) employed a mixture of deionized water and anhydrous ethanol as a solvent to hydrolyze the silane coupling agent KH550, and a quartz sand filter was soaked in the hydrolysate for modification. This method reduced the water wetting weight in the packed bed from 1.5589 g to 0.0607 g and effectively improved the oil removal efficiency. However, this method has disadvantages such as the large agent dosage requirement, environmental unfriendliness, and a low primary modification rate, which make it unsuitable for industrial mass production.

In this work, two different coupling agents, isopropyl dioleic (dioctylphosphate) titanate (DN101) and 3-methacryloxypropyl trimethoxy silane (KH570), were selected, and an improved modification method was employed to modify the quartz sand filter medium, where the coupling agent dosage was less than 10% of that used in the method proposed by Wei *et al.* (2013). This has advantages such as a low agent dosage requirement and suitability for mass production. In the following sections, the unmodified quartz filter medium and the filter media with the DN101 modification and KH570 modification are denoted as UQS, MQD-Ti and MQD-Si, respectively. In this paper, the wettability and oil removal performance of the three filter media were investigated. Here, the oil removal performance includes the oil removal efficiency and water head loss across the filter bed (Shin 2006). The oil removal efficiency (E) is calculated as

$$E = \frac{C_{in} - C_{out}}{C_{in}} \quad (1)$$

where C_{in} and C_{out} denote the inlet and outlet oil concentrations of the wastewater, mg/L.

To conduct comprehensive research on the filter bed oil removal performance, the quality factor (QF) defined by Brown (1993) and Kulkarni *et al.* (2012) was used:

$$QF = \frac{-\ln(1 - E)}{H} \quad (2)$$

where H is the water head loss, m.

MATERIALS AND METHODS

Materials and reagents

The quartz sand filter medium is from *Henan Songxing Filter Plant*, China. The DN101 and KH570 are from *Nanjing Pinning Coupling Agent Co., Ltd.*, China. The deionized water was prepared in the lab. The isopropanol, anhydrous ethanol and nitric acid were analytical-grade reagents. The gasoline engine oil SD40 is from *PetroChina Lubricant Company*, China. The SHR-5 mixer is from *Laizhou Xingge'er Chemical Plastics Machinery Co., Ltd.*, China.

Modification

The quartz sand filter sample (0.55–0.83 mm) was sieved via a 20–30 mesh stainless steel sieve, then boiled in deionized water for 30 min and repeatedly rinsed in deionized water until it was clean. Then, it was baked in a vacuum drying cabinet at 110°C for 12 h. After it cooled down, the quartz sand filter medium was soaked in a 1 mol/L nitric acid solution for 24 h and then in anhydrous ethanol for 30 min. Finally, it was washed and dried as a preprocessed quartz sand filter medium.

Isopropanol was employed as the solvent for the DN101 alcoholysis. The DN101 dosage was adjusted to prepare DN101 solutions with various concentrations that were subjected to magnetic mixture hydrolysis in a 20°C thermostatic water bath to obtain DN101 alcoholysis solutions. A mixed solvent of water-alcohol was used as the solution for the KH570 hydrolysis at 60°C to obtain the KH570 hydrolysate (Ma *et al.* 2008).

A certain amount of the preprocessed quartz sand filter medium was placed in the mixer, mixed at 300 rev/min and heated at 60°C for 5 min. Next, 1.2% of the filter medium weight of the DN101 alcoholysis solution (for MQD-Si, 1.5% KH570 hydrolysis solution) was sprayed slowly from the inlet onto the filter surface. The filter was kept in the dry state, mixed for another 70 min (50 min for MQD-Si), then cooled and soaked in water for 24 h, washed three times and dried at 100°C to a constant weight to prepare the MQD-Ti (or MQD-Si) filter medium.

Modification mechanism

Both the alcoholyzed DN101 and hydrolyzed KH570 contain hydroxyl groups. The condensation reaction between these hydroxyl groups and the hydroxyl groups on the quartz sand filter surface grafts the organic long-chain functional group of the coupling agent to the filter surface. The reaction equation is as follows (Zhang *et al.* 2013):

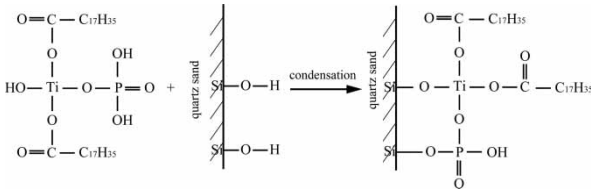

(3)

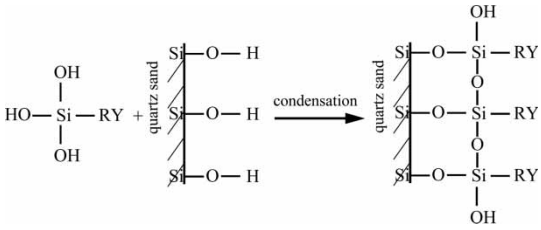

(4)

In Equation (4), RY represents

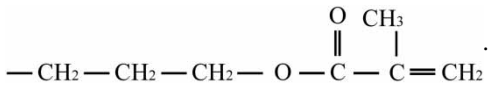

.

Wettability test

In a porous packing bed with a solid grain filling, when the capillary rise reaches the equilibrium state, the relation between the liquid weight in the capillary bed and the wetting contact angle is (Qing *et al.* 2009)

$$\cos\theta = \frac{g w_e r_s}{2\gamma_{GL}\pi R^2 \varepsilon} \tag{5}$$

where θ is the static contact angle of the wetting liquid on the filter surface, °; g is the gravitational acceleration, m/s^2; r_s is the effective radius of the porous packing bed, m; R is the inner diameter of the packing bed, m; ε is the packing bed porosity, %; w_e is the liquid mass that enters the capillary when the capillary rise reaches the equilibrium state, g; and γ_{GL} is the surface tension of the wetting liquid, mN/m.

As it is difficult to measure r_s, the contact angle cannot be calculated directly via Equation (5). Yang & Chang (2008) proposed a concept of the Lipophilic to Hydrophilic Ratio (LHR) as follows:

$$\mathrm{LHR} = \frac{\cos\theta_O}{\cos\theta_W} \tag{6}$$

where θ_O and θ_W are the wetting contact angles of oil and water, respectively, for a single sample.

Substituting Equation (5) into Equation (6):

$$\mathrm{LHR} = \frac{g w_{eO} r_s}{2\gamma_O \pi R^2 \varepsilon} \Big/ \frac{g w_{eW} r_s}{2\gamma_W \pi R^2 \varepsilon} = \frac{w_{eO}\gamma_W}{w_{eW}\gamma_O} \tag{7}$$

where w_{eO} and w_{eW} are the liquid mass that enters the capillary when the capillary ascent reaches the equilibrium state, g.

In this paper, cyclohexane represents the oil phase, and deionized water represents the water phase. At 20°C, the surface tensions of cyclohexane and water are 25.5 mN/m and 72.8 mN/m, respectively. For the detailed test procedure, please refer to Qing *et al.* (2009). Experiments were run in triplicate and the error bar corresponds to one standard deviation.

Filtration experimental setup

The filtration apparatus is shown in Figure 1. The filtration column is a Plexiglas tube with a height of 2,000 mm. The height of the pebble supporting layer is 300 mm, the height of the filter medium layer is 900 mm, and the inner diameter of the filtration column is 33 mm. During filtration, the inflow pump is opened, and the surplus water flows out via an overflow tube to maintain a steady water level in the filtering pool. A flow meter was installed in the water outlet pipe and constantly adjusted during the filtration process to maintain a steady effluent flow. To compare the filtration effects of different filter media, three filtration columns were set up with the same operating conditions (temperature of 25 ± 1°C, initial oil concentration of 17.3 mg/L and face velocity of 4 m/h).

Wastewater with emulsified oil was prepared. The engine oil SD40 was the raw material, and ultrasonic

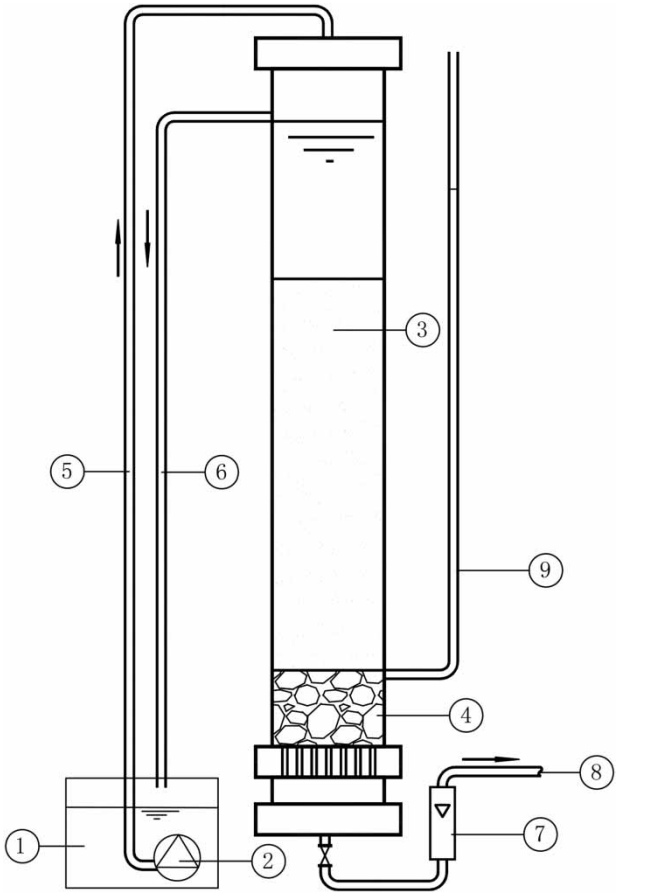

Figure 1 | Schematic diagram of the filtration apparatus. (1) Emulsified oily wastewater tank. (2) Inflow pump. (3) Filtration column. (4) Filter supporting bed. (5) Inflow pipe. (6) Overflow pipe. (7) Flow meter. (8) Effluent. (9) Piezometric tube.

emulsification and mechanical mixing were employed to prepare the oil/water emulsion (Kamogawa *et al.* 2001; Lin & Chen 2006). After the prepared emulsified oil was stood for 24 h, the oil concentration variation was <10% (Zhou *et al.* 2008), and the oil droplet size was stabilized in the range of 1–10 μm.

Characterization

Field emission scanning electron microscopy (JSM-5600LV, JEOL, Japan) was employed to characterize the morphology and structure. The chemical composition of the filter media was measured by a Fourier transformation infrared (FTIR) spectrometer (IFS66 V/S, BRUKER, Germany), and the surface composition was analyzed via X-ray photoelectron spectroscopy (XPS) (VG ESCALAB 210, VG Scientific).

RESULTS AND DISCUSSION

Wettability characterization

Figure 2 shows the wetting weights of cyclohexane and water for the three filter media and their LHR values. MQD-Ti has a slightly larger cyclohexane wetting weight than UQS or MQD-Si, and UQS has a significantly larger water wetting weight than the other two filtering media (MQD-Si followed by MQD-Ti in descending order). This means that the coupling agent effectively enhances the hydrophobicity and lipophilicity on the quartz sand filter surface. The three quartz sand filter media in descending order of LHR and hydrophobicity were MQD-Ti > MQD-Si > UQS. This means that the chain length of the coupling agent organic functional group affects the filter surface wettability, with a longer carbon chain resulting in stronger hydrophobicity. After modification, the quartz sand filter LHR increased from 1.31 (UQS) to 12.09 (MQD-Ti) and 5.11 (MQD-Si).

Filtration performance

Figure 3 shows filtration efficiency for the three filter media. In the first 9 h, the removal efficiency essentially stabilizes. Based on assumptions made by previous researchers (Wurster *et al.* 2015), with the continuous inflow of oily

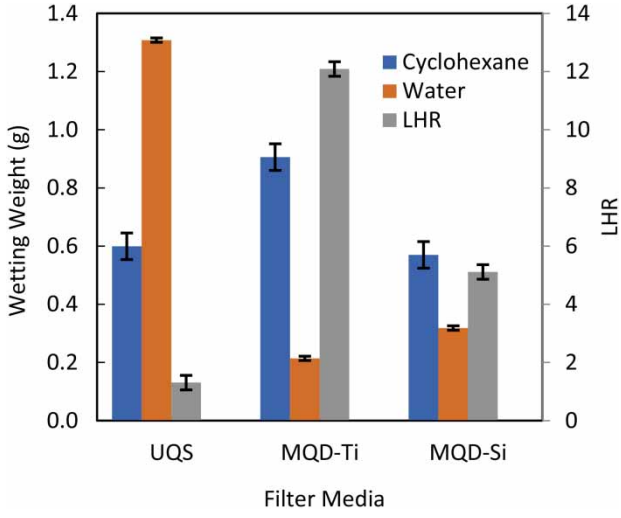

Figure 2 | Cyclohexane and water wetting weights and LHR values of three samples.

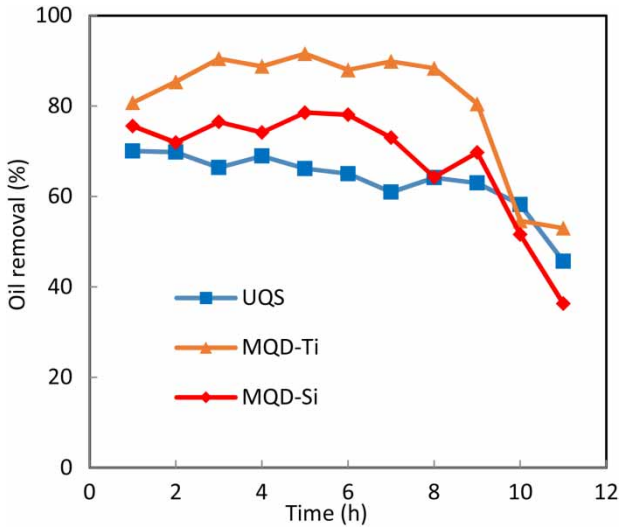

Figure 3 | Oil removal efficiency as a function of time for the three samples.

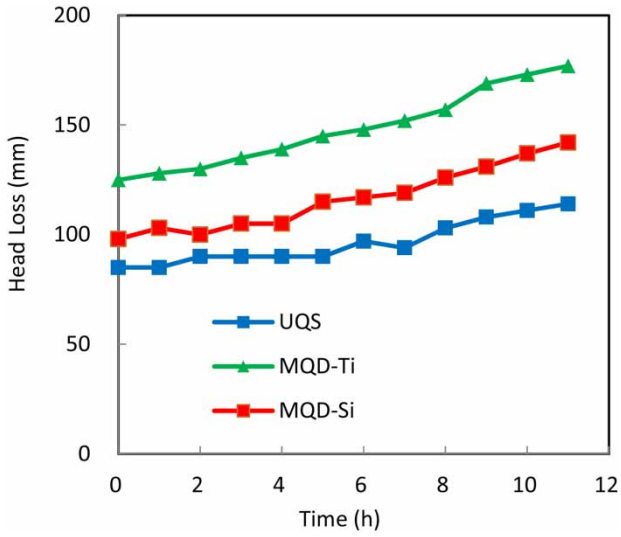

Figure 4 | Water head loss as a function of time for the three samples.

wastewater, the inflowing oil droplets coalesce with the oil entrapped in the filtering bed, and thereby, oil is steadily removed. As a larger LHR means better oil wettability on the filter medium surface, oil is more likely to be adsorbed on the filter surface, and therefore, the oil removal efficiency is higher. The oil removal efficiencies of the three filter media in descending order are MQD-Ti > MQD-Si > UQS, which matches the order of their LHR values. During this period, the average UQS oil removal efficiency is 66.0%, and the oil removal efficiencies of MQD-Ti and MQD-Si reach 87.1% and 73.5%, which are 21.1% and 7.5% improvements, respectively, over that of UQS. After 9 h, the oil removal efficiency starts to decline. This is because after oil is adsorbed on the filter surface, the channels between the filter media are blocked. When the face velocity is fixed, the water head loss in the filter bed increases (as shown in Figure 4), and the media velocity increases. Therefore, the water flow shear force on the oil adhering to the filter surface increases, and the service cycle is then complete.

Figure 4 shows that filter media with different LHR values have different water head losses during the initial period of filtering. A stronger hydrophobicity results in a higher water head loss, which is consistent with a research finding by Huang & Lim (2006). When the filter medium surface hydrophobicity is strong, water is less likely to approach the filter medium surface (Choi & Kim 2006; Chu *et al.* 2017). Therefore, the water channels in the filtering bed are reduced, which leads to an increase in the water head loss. In general, MQD-Ti has the highest filtering bed water head loss, while UQS has the lowest. It can be seen from Figures 3 and 4 that the stronger the hydrophobicity of the filter medium, the more entrapped oil accumulates in the filter bed, the proportion of voids in the filter bed then becomes smaller and the water head loss increase rate becomes faster. Therefore, the MQD-Ti filtering bed water head loss increase rate is the highest, while UQS has the slowest increasing rate.

A combined performance measure of the oil removal efficiency and water head loss is given by the quality factor in Equation (1). Figure 5 shows the quality factor values of the three filter media. Before 6 h, the quality factor values of the three filter media were stable. The average value for MQD-Ti was 0.668 m^{-1}, far exceeding those of the other two. The quality factor value of MQD-Si was slightly higher than that of UQS, 0.575 m^{-1} versus 0.564 m^{-1}. This means that as the LHR increases, the quality factor increases faster. After 6 h, the quality factor values of the three filters started to decline, with MQD-Ti and MQD-Si exhibiting faster declining rates than UQS. This is because when more oil is entrapped in the MQD-Ti and MQD-Si filter beds, the filter channel blockage is more

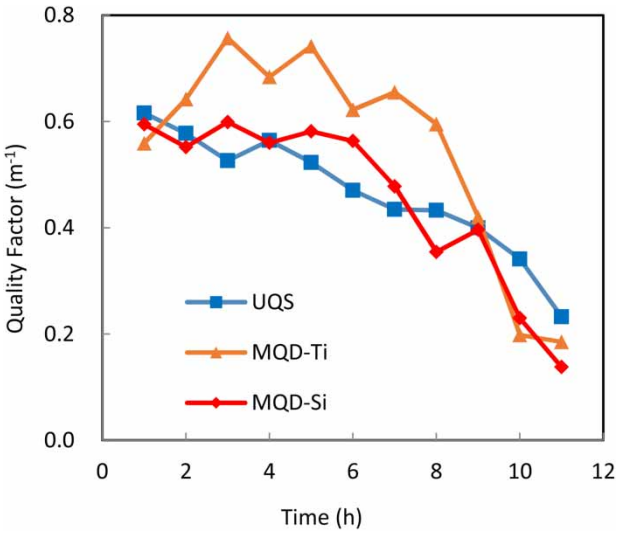

Figure 5 | Quality factor as a function of time for the three samples.

severe, the filter water head loss increases faster and the quality factor thereby declines faster.

SEM analysis

SEM diagrams of the three filter media are shown in Figure 6. The shapes and structures of the three filter media are similar and irregular. This means that the shape and structure of the filter are not altered by the modifications. UQS has a coarse surface, numerous edges, an irregular arrangement and multiple grooves and craters, which demonstrate an apparent crystalline structure, anisotropic characteristics and underdeveloped surface porosity. MQD-Ti and MQD-Si have a large number of fine grains due to their characteristics of underdeveloped surface porosity and a coarse surface.

FTIR analysis

Infrared spectra of the three filter media are shown in Figure 7. For UQS, there is a hydroxyl group absorption peak at 3,734 cm^{-1} (Fang *et al.* 2008). The concentration zones at 1,200–1,100 cm^{-1} and 472 cm^{-1} represent antisymmetric stretching vibrations and bending vibrations of Si-O-Si, and the absorption peaks near 3,415 cm^{-1} and at 1,627 cm^{-1} represent stretching vibrations and bending vibrations of the quartz sand surface adsorption water O-H. Near 3,415 cm^{-1}, the quartz sand surface Si-OH stretching vibrations and water molecule stretching vibrations overlap, which widens the absorption peak at this point. For MQD-Ti, the C-H and C-C characteristic absorption peaks are at 2,918 cm^{-1} and 2,857 cm^{-1}, respectively, which are DN101 absorption peaks. The C-H bending vibration occurs at 1,450 cm^{-1}, and the stretching vibration peak of ester C = O occurs at 1,726 cm^{-1}. By comparison, UQS has no characteristic absorption peaks for these groups; the hydroxyl group absorption peak at 3,734 cm^{-1} on the quartz sand surface disappears after modification. This means that this hydroxyl group reacts with DN101 (Fang *et al.* 2008). For KH570, the C-H stretching vibration characteristic peaks that belong to KH570 -CH_2 and -CH_3 occur at 2,852 cm^{-1} and 2,926 cm^{-1}, respectively. At 1,791 cm^{-1}, there is a C = O low-frequency stretching vibration absorption peak, and at 1,539 cm^{-1}, there is a C = C bending vibration absorption peak. This means that the silane coupling agent KH570 develops a chemical bond to the quartz sand filter surface. Due to the small dosage of the coupling agent, although the absorption peaks of the other organic functional groups in the coupling agent are invisible, a chemical bonding reaction between DN101, KH570 and the quartz sand surface may still exist.

XPS analysis

The XPS spectra of the three filters are shown in Figure 8. UQS mainly consists of two elements, O (532.8 eV) and Si (103.5 eV), whose atomic concentrations are 69.55% and 30.45%, respectively. The MQD-Ti surface contains O (536.4 eV), Si (102.8 eV), C (284.8 eV) and a small portion of Ti (468.4 eV), with atom concentrations of 40.93%, 16.76%, 41.46% and 0.85%, respectively. The MQD-Si sample mainly consists of Si (107.6 eV), C (290.0 eV) and O (536.8 eV), with atom concentrations of 12.27%, 31.81% and 55.92%, respectively. Compared with UQS, after the modification, the Si concentration on the quartz sand filter surface declines significantly. The reason for this is that when the coupling agent bonds to the filter surface, the surface is covered. This proves that the coupling agent is successfully grafted to the filter surface.

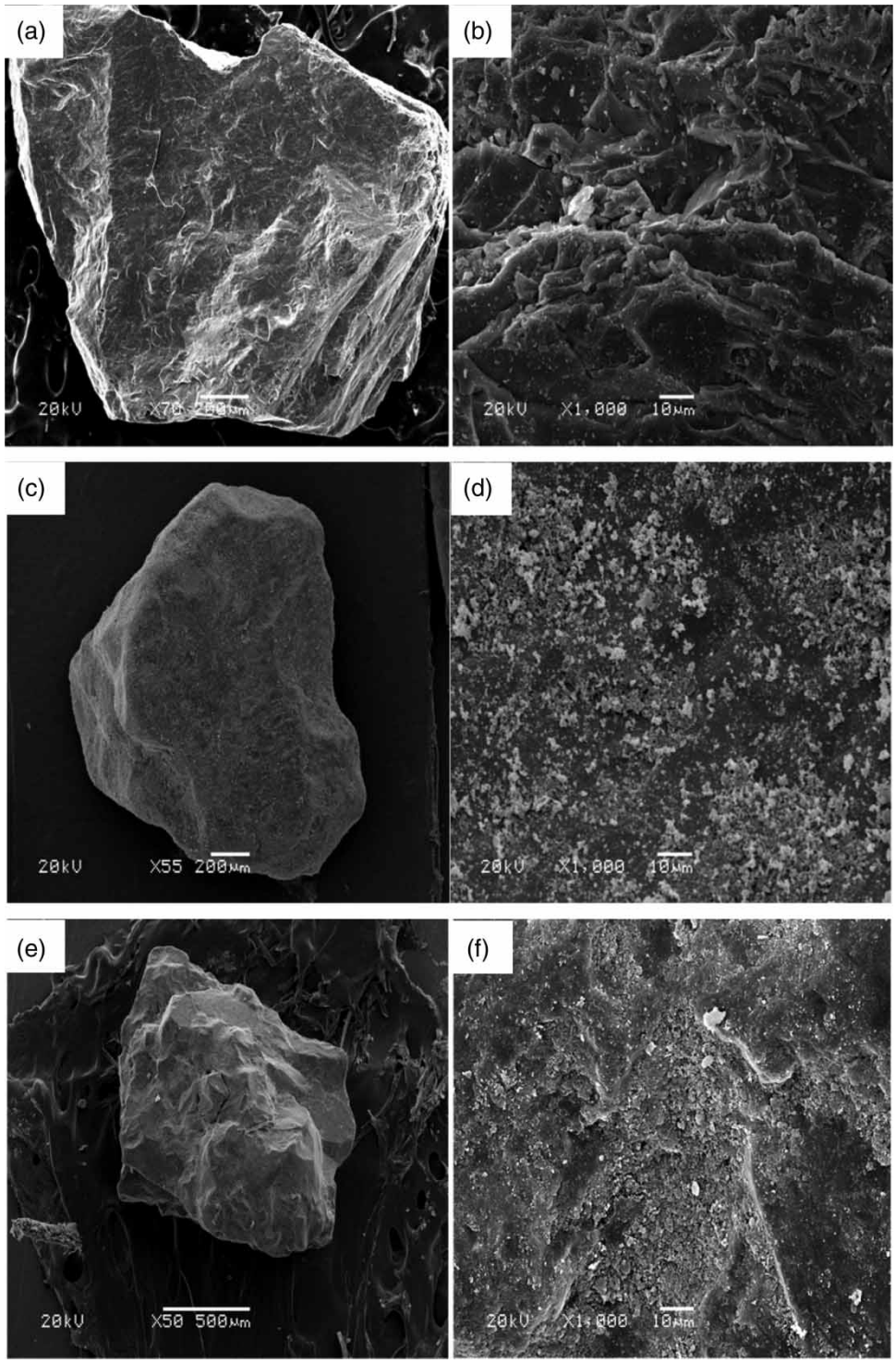

Figure 6 | SEM micrographs of (a) and (b) UQS, (c) and (d) MQD-Ti and (e) and (f) MQD-Si.

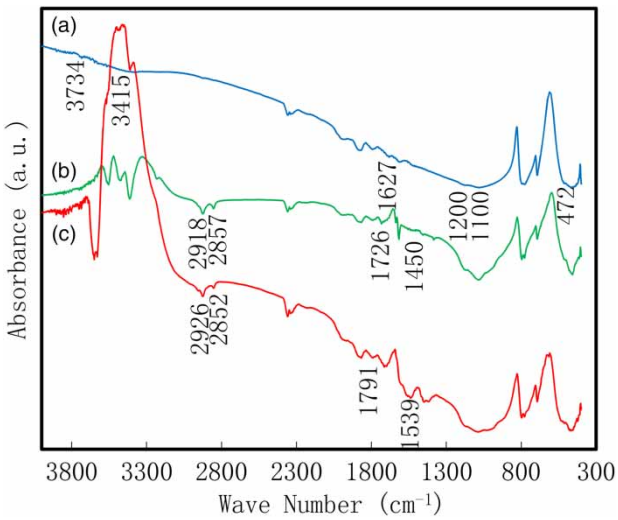

Figure 7 | FTIR spectra of (a) UQS, (b) MQD-Ti and (c) MQD-Si.

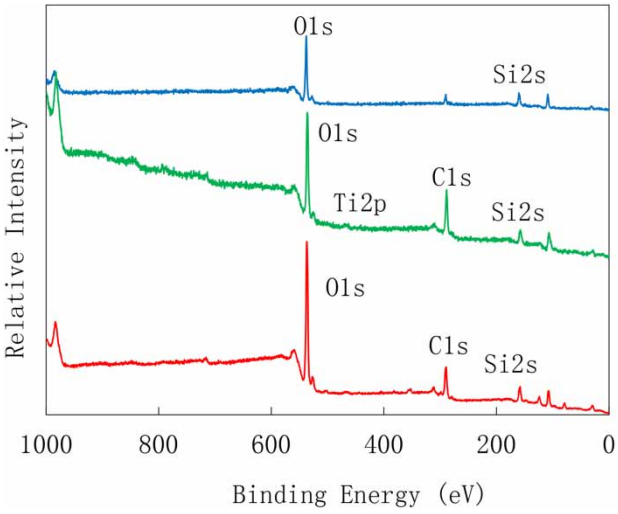

Figure 8 | XPS spectra of (a) UQS, (b) MQD-Ti and (c) MQD-Si.

CONCLUSION

As the coupling agent contains a long-chain organic functional group and a short chain alkoxy capable of hydrolysis or alcoholysis, a condensation reaction occurs between the hydrolysis- or alcoholysis-generated hydroxyl groups and the hydroxyl groups on the quartz sand filter medium surface. The long-chain organic functional group is grafted to the filter medium surface, and thereby, the hydrophobicity and lipophilicity of the filter medium are increased. FTIR and XPS analyses show that after modification, organic functional groups unique to the coupling agent appear on the filter medium surface. This indicates that the modification is successful. After the surface modification, the oil removal efficiency and quality factor are effectively improved; the oil removal efficiencies of MQD-Ti and MQD-Si improve by 21.1% and 7.5% over that of UQS. To summarize, the hydrophobicity modification effectively improves the oil removal efficiency.

ACKNOWLEDGEMENTS

This work was supported by the National Natural Science Foundation of China (No. 51668032) and Foundation of A Hundred Youth Talents Training Program of Lanzhou Jiaotong University (No. 152022).

REFERENCES

Bai, R. & Tien, C. 1997 Particle detachment in deep bed filtration. *Journal of Colloid and Interface Science* **186** (2), 307–317.

Bai, R. & Tien, C. 2000 Effect of deposition in deep-bed filtration: determination and search of rate parameters. *Journal of Colloid and Interface Science* **231** (2), 299–311.

Brown, R. C. 1993 *Air Filtration: An Integrated Approach to the Theory and Applications of Fibrous Filters.* Oxford, Pergamon.

Choi, C.-H. & Kim, C.-J. 2006 Large slip of aqueous liquid flow over a nanoengineered superhydrophobic surface. *Physical Review Letters* **96** (6), 066001.

Chu, F., Wu, X., Zhu, Y. & Yuan, Z. 2017 Relationship between condensed droplet coalescence and surface wettability. *International Journal of Heat and Mass Transfer* **111**, 836–841.

Fang, X.-Y., Wang, T.-J., Wu, H.-X. & Jin, Y. 2008 Surface chemical modification of nanosized oxide particles with a titanate coupling reagent in isopropanol. *Industrial & Engineering Chemistry Research* **47** (5), 1513–1517.

Hamoda, M., Al-Ghusain, I. & Al-Mutairi, N. 2004 Sand filtration of wastewater for tertiary treatment and water reuse. *Desalination* **164** (3), 203–211.

Huang, X. & Lim, T.-T. 2006 Performance and mechanism of a hydrophobic–oleophilic kapok filter for oil/water separation. *Desalination* **190** (1), 295–307.

Jamaly, S., Giwa, A. & Hasan, S. W. 2015 Recent improvements in oily wastewater treatment: progress, challenges, and future opportunities. *Journal of Environmental Sciences* **37**, 15–30 doi:http://dx.doi.org/10.1016/j.jes.2015.04.011.

Kamogawa, K., Akatsuka, H., Matsumoto, M., Yokoyama, S., Sakai, T., Sakai, H. & Abe, M. 2001 Surfactant-free O/W emulsion formation of oleic acid and its esters with ultrasonic dispersion. *Colloids and Surfaces A: Physicochemical and Engineering Aspects* **180** (1), 41–53.

Kota, A. K., Kwon, G., Choi, W., Mabry, J. M. & Tuteja, A. 2012 Hygro-responsive membranes for effective oil-water separation. *Nature Communications* **3**, 1025.

Kratochvil, M. J., Manna, U. & Lynn, D. M. 2017 Superhydrophobic polymer multilayers for the filtration-and absorption-based separation of oil/water mixtures. *Journal of Polymer Science Part A: Polymer Chemistry* **55** (18), 3127–3136.

Kulkarni, P. S., Patel, S. U. & Chase, G. G. 2012 Layered hydrophilic/hydrophobic fiber media for water-in-oil coalescence. *Separation and Purification Technology* **85**, 157–164.

Li, Y., Gong, H., Dong, M. & Liu, Y. 2016 Separation of water-in-heavy oil emulsions using porous particles in a coalescence column. *Separation and Purification Technology* **166**, 148–156.

Lin, C.-Y. & Chen, L.-W. 2006 Emulsification characteristics of three-and two-phase emulsions prepared by the ultrasonic emulsification method. *Fuel Processing Technology* **87** (4), 309–317.

Ma, S.-r., Shi, L.-y., Feng, X., Yu, W.-j. & Lu, B. 2008 Graft modification of ZnO nanoparticles with silane coupling agent KH570 in mixed solvent. *Journal of Shanghai University (English Edition)* **12** (3), 278–282.

Mazumdar, M., Jammoria, A. S. & Roy, S. 2017 Effective rates of coalescence in oil–water dispersions under constant shear. *Chemical Engineering Science* **157**, 255–263.

Mueller, J., Cen, Y. & Davis, R. H. 1997 Crossflow microfiltration of oily water. *Journal of Membrane Science* **129** (2), 221–235.

Ngang, H., Ahmad, A., Low, S. & Ooi, B. 2017 Preparation of thermoresponsive PVDF/SiO 2-PNIPAM mixed matrix membrane for saline oil emulsion separation and its cleaning efficiency. *Desalination* **408**, 1–12.

Qing, C., Bigui, W. & Yingdong, H. 2009 Capillary pressure method for measuring lipophilic hydrophilic ratio of filter media. *Chemical Engineering Journal* **150** (2), 323–327 doi: http://dx.doi.org/10.1016/j.cej.2009.01.005.

Shin, C. 2006 Filtration application from recycled expanded polystyrene. *Journal of Colloid and Interface Science* **302** (1), 267–271.

Shin, C. & Chase, G. 2004 The effect of wettability on drop attachment to glass rods. *Journal of Colloid and Interface Science* **272** (1), 186–190.

Takahashi, T., Miyahara, T. & Nishizaki, Y. 1979 Separation of oily water by bubble column. *Journal of Chemical Engineering of Japan* **12** (5), 394–399.

Wei, B., Chang, Q., Bao, C., Dai, L., Zhang, G. & Wu, F. 2013 Surface modification of filter medium particles with silane coupling agent KH550. *Colloids and Surfaces A: Physicochemical and Engineering Aspects* **434**, 276–280.

Wurster, S., Kampa, D., Meyer, J., Müller, T., Mullins, B. & Kasper, G. 2015 Measurement of oil entrainment rates and drop size spectra from coalescence filter media. *Chemical Engineering Science* **132**, 72–80.

Yang, B. & Chang, Q. 2008 Wettability studies of filter media using capillary rise test. *Separation and Purification Technology* **60** (3), 335–340.

Zhang, J., Guo, Z., Zhi, X. & Tang, H. 2013 Surface modification of ultrafine precipitated silica with 3-methacryloxypropyltrimethoxysilane in carbonization process. *Colloids and Surfaces A: Physicochemical and Engineering Aspects* **418**, 174–179.

Zhou, Y.-B., Tang, X.-Y., Hu, X.-M., Fritschi, S. & Lu, J. 2008 Emulsified oily wastewater treatment using a hybrid-modified resin and activated carbon system. *Separation and Purification Technology* **63** (2), 400–406.

Zhou, Y., Tang, X., Xu, Y. & Lu, J. 2010 Effect of quaternary ammonium surfactant modification on oil removal capability of polystyrene resin. *Separation and Purification Technology* **75** (3), 266–272.

First received 28 August 2017; accepted in revised form 17 December 2017. Available online 5 January 2018